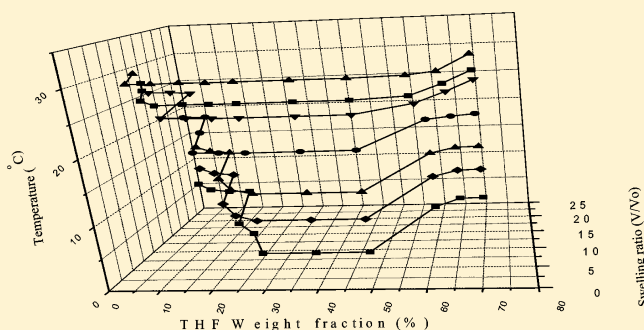


# Molecular Thermodynamic Analysis for Assessing the Relationship Between Reentrant Swelling Behavior and Ternary Liquid–Liquid Equilibrium for Poly(*N*-isopropylacrylamide) Nanometer-Sized Gel Particles in a Water–Tetrahydrofuran Cosolvent System

Sang Chul Jung and Young Chan Bae\*

Division of Chemical Engineering and Molecular Thermodynamics Laboratory, Hanyang University, Seoul 133-791, Korea

**ABSTRACT:** The influence of phase separation on swelling behavior was investigated based on the thermodynamic framework of reswelling phenomena. The cloud-point for a ternary system of water(1)–tetrahydrofuran (THF)(2)–poly(*N*-isopropylacrylamide)(3) was examined by thermo-optical analysis (TOA). Nanometer-sized *N*-isopropylacrylamide (NIPA) gel particles were prepared by precipitation polymerization, and their swelling behaviors were determined using photon correlation spectroscopy (PCS). NIPA gel particles underwent reswelling when the ratio of water to THF was varied. First, the modified double lattice model (MDL) was employed to determine ternary interaction energy parameters for the liquid–liquid equilibrium (LLE) of linear poly-NIPA in a water–THF cosolvent system. The reentrant swelling equilibria of the NIPA gel in the water–THF system were then calculated using the interaction energy parameters.



## 1. INTRODUCTION

The swelling of hydrogel networks in response to environmental stimuli has been exploited in a variety of applications for the past few decades. The swelling properties of hydrogels can be controlled by varying temperature,<sup>1,2</sup> pH,<sup>3,4</sup> system composition,<sup>5–8</sup> salt concentration,<sup>9,10</sup> or the type of surfactant,<sup>11</sup> and the use of these stimuli responses have been proposed for applications such as controlled drug delivery,<sup>12,13</sup> polymeric membranes,<sup>14</sup> and the separation and purification of fluid mixtures.

In the field of chemical engineering, the thermodynamic model for calculating swelling phenomena is particularly important in chemical process design for industrial applications. Significant attention has been focused on the reentrant swelling behavior of hydrogels since this is an unusual feature of gel network reswelling when the solvent concentration or temperature of the system is changed.<sup>15–23</sup> The reentrant swelling phenomena was first experimentally demonstrated by Katayama et al.<sup>5</sup> for a *N*-isopropylacrylamide (NIPA) gel in a mixed organic and water solvent, and qualitatively interpreted in terms of the attractive interactions between water and solvent molecules. The reentrant swelling behaviors of gels were further investigated by Amiya et al.<sup>15</sup> and Hirotsu.<sup>16</sup> They theoretically applied the binary solvent effect to the swelling behaviors induced by a pseudosingle solvent. Makae et al.<sup>19,20</sup> also investigated the reentrant swelling behavior of NIPA gel in a mixed solvent. They reported that the reentrant swelling of the gel was strongly dependent on the properties of the mixed solvent as well as intermolecular interactions in the polymer

network. Gundogan and Okay<sup>24</sup> predicted the reentrant swelling behavior using the Flory–Huggins interaction parameter in the gel network. Lele et al.<sup>25</sup> also predicted the reentrant swelling phenomena in terms of a thermodynamic model based on lattice fluid theory.

A thermodynamic framework exists for interpreting the swelling equilibria in terms of the interactions between the polymer and solvent. Oliveira et al.<sup>26</sup> presented a quasi-chemical model that explained the competition between hydrogen bonding and dispersion forces, leading to the transition from less entropic swollen gel phases to more entropic collapsed gel states. Prange et al.<sup>27</sup> also identified interaction energy parameters from liquid–liquid equilibrium (LLE) for a linear poly-NIPA (PNIPA)–water system using an oriented quasi-chemical model and applied these parameters to the swelling equilibria of the gel. Cussler et al.<sup>28,29</sup> introduced the Sanchez–Lacombe lattice-fluid model, which considered holes in the lattice as a component in the free energy of mixing and compared the model with their swelling data. Moerkerke et al.<sup>30</sup> suggested a simple model in which the polymer–solvent interaction parameter depends not only on the temperature but also on the polymer concentration. Recently, the swelling behavior of hydrogels in ternary systems has attracted increased attention. Nandi and Winter<sup>31</sup> predicted the swelling phenomena of a partially cross-linked polymer using a ternary

Received: October 2, 2011

Revised: January 9, 2012

Published: January 12, 2012



Table 1. Experimental Cloud-Point Data for PNIPA in Mixed Solvents

weight fraction			cloud-point	weight fraction			cloud-point
water(1)	THF(2)	PNIPA(3)		water(1)	THF(2)	PNIPA(3)	
0.417	0.527	0.026	20 °C	0.839	0.156	0.004	20 °C
0.415	0.512	0.042		0.819	0.143	0.037	
0.383	0.501	0.095		0.788	0.124	0.086	
0.339	0.492	0.149		0.774	0.118	0.108	
0.355	0.535	0.110		0.899	0.109	0.002	
0.311	0.534	0.155	28 °C	0.888	0.088	0.024	28 °C
0.295	0.544	0.161		0.851	0.086	0.765	
0.301	0.530	0.169		0.825	0.083	0.092	
0.303	0.542	0.155		0.806	0.070	0.124	
0.351	0.608	0.041		0.943	0.052	0.005	
0.312	0.561	0.127	32 °C	0.905	0.049	0.045	32 °C
0.289	0.540	0.171		0.899	0.041	0.059	

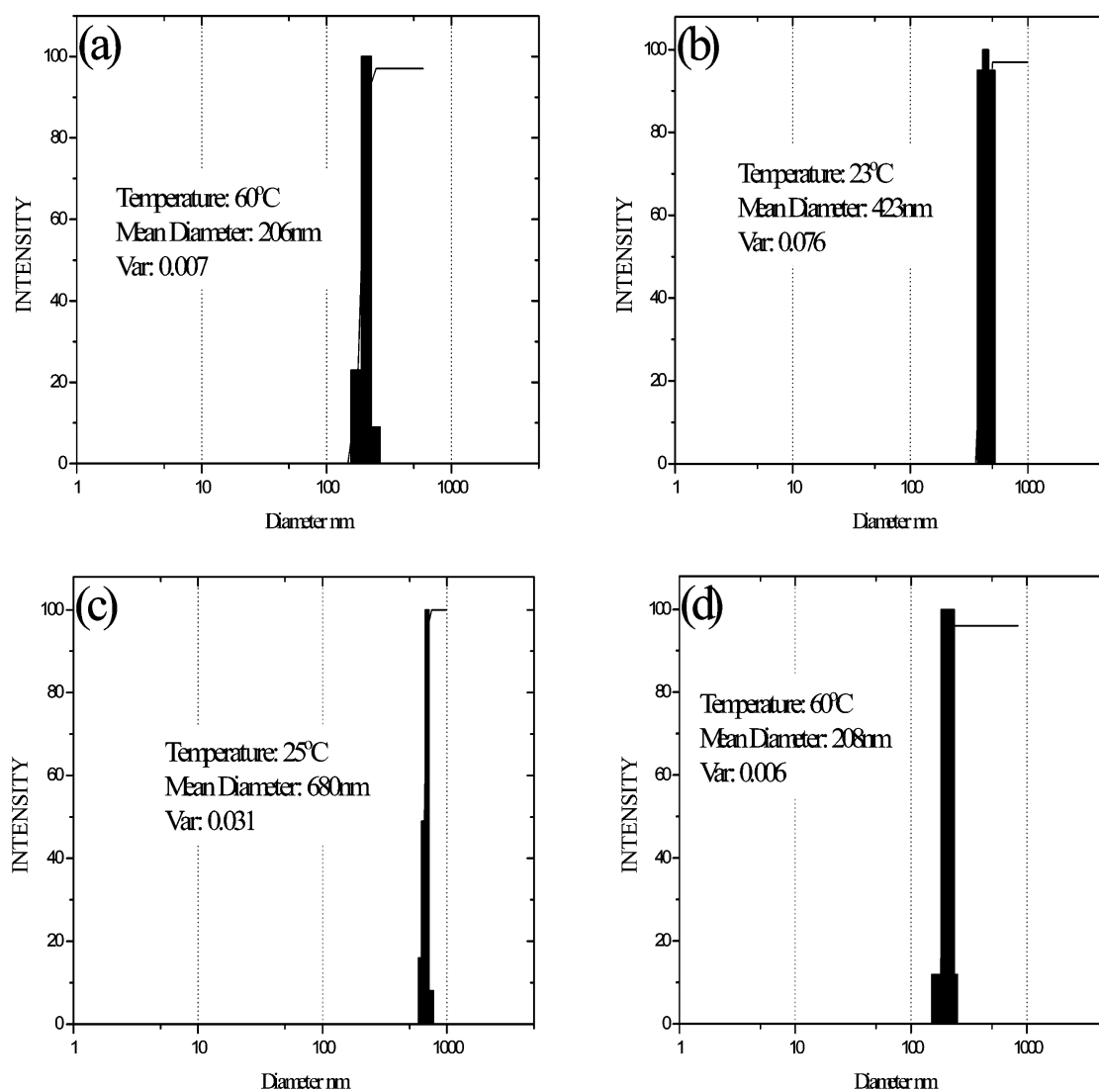


**Figure 1.** The size distribution of NIPA gel particles with various conditions. (a,b) Particle distributions of the THF weight fraction of 15%. (c,d) Particle distributions of the THF weight fraction of 70%.

thermodynamic model. Zhi et al.<sup>32</sup> predicted the swelling behavior of hydrogel in water–ethanol mixtures with a thermodynamic model. Okeowo and Dorgan<sup>33</sup> calculated the multicomponent swelling equilibria with various cross-linking densities using the Flory–Huggins interaction parameter.

In the present study, the effects of solvent composition and solution conditions on the swelling properties of NIPA hydrogels were examined at various temperatures. Because the rate of response of a given hydrogel is inversely proportional to the square of the size of the gel, we prepared

a nanometer-sized NIPA gel, thereby enabling the measurement of quick and uniform responses.<sup>34</sup> We extended MDL theory to calculate the reentrant volume transition of a polymeric gel in a mixture of two solvents. The parameters between components obtained from the ternary phase equilibrium data for water(1)–tetrahydrofuran (THF)(2)–linear PNIPA(3) were used to thermodynamically interpret the reentrant swelling phenomena of water(1)–THF(2)–cross-linked NIPA gel(3). Calculated swelling equilibria were compared to the swelling behavior observed experimentally when gels were prepared via precipitation polymerization. The binary system was successfully described by the modified double lattice (MDL) model in previous studies,<sup>35–37</sup> and network elasticities were described using the Flory–Erman theory,<sup>38</sup> which considers nonaffine displacements of the network junctions under a high degree of swelling. The energy parameters in the resulting swelling model were determined from ternary phase equilibrium data. Using those energy parameters, calculated reentrant swelling behaviors were compared with experimentally observed swelling data for water(1)–THF(2)–cross-linked NIPA gels(3).

## 2. EXPERIMENTAL SECTION

### 2.1. Measurements of the Ternary Phase Diagram.

The cloud-point curve of the water(1)–THF(2)–PNIPA(3) ternary system was determined by thermo-optical analysis (TOA). A TOA apparatus consisting of a polarizing microscope (OLYMPUS BX40), a heating–cooling stage, a photodiode (Mettler FP 82), a microprocessor (Mettler FP 90), and a PC was used for data acquisition. The heating and cooling stage was designed to enable the observation of the thermal behavior of a sample. PNIPA samples ( $M_n = 20\,000$ – $25\,000$ ) were obtained from Sigma-Aldrich. Phase diagram samples were prepared in separate test tubes, and the composition of each sample was gravimetrically measured. Each solution was stirred for approximately 4 h, after which time the solution was transferred to a Pyrex tube (i.d. 1 mm and o.d. 3 mm). The test tube was then sealed under dry nitrogen gas using a natural gas/oxygen flame with a sufficiently high temperature such that the Pyrex tube could be sealed in less than 2 s. Cloud-points with weight fractions of the polymer solutions were measured as described by Bae et al.<sup>39</sup> (Table 1).

**2.2. Measurement of the Swelling Behavior of a Nanosized Gel via Photon Correlation Spectroscopy (PCS).** NIPA (MW = 113.16) was obtained from Sigma-Aldrich Co. and recrystallized before use.  $N,N'$ -Methylenebisacrylamide and ammonium persulfate were used as a cross-linker and initiator, respectively. A nonionic surfactant, TWEEN 20, was used to prevent aggregation among the particles. The gel particles were prepared by precipitation polymerization at 70 °C for 4 h under nitrogen.<sup>40</sup> Distilled deionized water was used as a solvent. The results of PCS measurement of gel particles are shown in Figure 1. For the various conditions, their variances were below 0.07. This confirms that our prepared particles are monodisperse.

The hydrodynamic diameters of the hydrogel particles in aqueous solution were measured by PCS with a 514.5 nm laser source at a 90° angle at various temperatures. The samples were filtered by a 0.45  $\mu\text{m}$  syringe filter. The scattered light intensities and time autocorrelation functions were collected using the CONTIN method<sup>41,42</sup> and were determined at various temperatures.

## 3. THEORETICAL CONSIDERATIONS

**3.1. Thermodynamic Model of Ternary Systems.** The Helmholtz energy of mixing was used in the form of the Flory–Huggins theory for polymer solutions that was extended to the three-component systems by Tompa<sup>43</sup> and Scott.<sup>44</sup> This expression is given by

$$\frac{\Delta_{\text{mix}}A}{N_r kT} = \sum_i \frac{\phi_i}{r_i} \ln \phi_i + \sum_{i,j} \chi_{\text{OB},ij} \phi_i \phi_j \quad (1)$$

where  $N_r (= \sum_{i=1}^3 N_r r_i)$  is the total number of lattice sites,  $k$  is the Boltzmann constant,  $r_i$  is the number of segments, and  $\phi_i (= N_r r_i / N_r)$  is the volume fraction of the  $i$ th component  $i$ . The binary interaction parameter  $\chi_{\text{OB}}$  is defined by

$$\chi_{\text{OB},ij} = C_\beta \left( \frac{1}{r_j} - \frac{1}{r_i} \right)^2 + \left( 2 + \frac{1}{r_j} \right) \tilde{\epsilon}_{ij} - \left( \frac{1}{r_j} - \frac{1}{r_i} + C_\gamma \tilde{\epsilon}_{ij} \right) \tilde{\epsilon}_{ij} \phi_j + C_\gamma \tilde{\epsilon}_{ij}^2 \phi_j^2, \quad i \neq j \quad (2)$$

where  $C_\beta$  and  $C_\gamma$  are universal constants with the values 0.1415 and 1.7986, respectively. These constants were determined based on correlations with the Monte Carlo simulation results reported by Madden et al.<sup>45</sup>

The chemical potentials of each component are required to generate the ternary coexistence curve, and can be determined using the following equation:

$$\frac{\Delta \mu_i}{kT} = \left[ \frac{\partial(\Delta A / N_r kT)}{\partial N_i} \right]_{T,V,N_{j \neq i}} \quad (3)$$

A coexistence curve can be calculated using the following conditions:

$$\Delta \mu_i' = \Delta \mu_i'' \quad (i = 1, 2, 3) \quad (4)$$

where the prime and double prime superscripts indicate two phases at equilibrium.

The spinodal and critical conditions required for the calculation of the ternary phase diagram can be derived from  $\Delta_{\text{mix}}A$  of eq 1 by the Gibbs method of determinants.<sup>46</sup> The spinodal condition is simply

$$D = A_{11}A_{22} - A_{12}^2 = 0 \quad 1 \leq i, j \leq 2 \quad (5)$$

where  $A_{ij}$  is defined as

$$A_{ij} = \left[ \frac{\partial^2(\Delta_{\text{mix}}A / N_r kT)}{\partial \phi_i \partial \phi_j} \right]_{T,V} \quad (6)$$

The derivatives of the spinodal determinant needed for substitution to form the critical determinant are then

$$D_1 = (\partial D / \partial \phi_1) = A_{111}A_{22} + A_{11}A_{221} - 2A_{12}A_{121} \quad (7a)$$

$$D_2 = (\partial D / \partial \phi_2) \\ = A_{112}A_{22} + A_{11}A_{222} - 2A_{12}A_{122} \quad (7b)$$

The critical condition (denoted by  $D^1$  and  $D^2$ ) can be written as either

$$D^1 \equiv \begin{vmatrix} D_1 & D_2 \\ A_{21} & A_{22} \end{vmatrix} = D_1A_{22} - D_2A_{12} = 0 \quad (8a)$$

or

$$D^2 \equiv \begin{vmatrix} A_{11} & A_{12} \\ D_1 & D_2 \end{vmatrix} = D_2A_{11} - D_1A_{12} = 0 \quad (8b)$$

**3.2. Elastic Contribution.** According to Flory,<sup>47</sup> the chemical potential of a solvent in a gel phase coexisting with a pure solvent is given by

$$\mu_1 - \mu_1^0 = \Delta\mu_1 = \Delta\mu_{1,\text{mix}} + \Delta\mu_{1,\text{ela}} \quad (9)$$

where  $\Delta\mu_{1,\text{mix}}$  and  $\Delta\mu_{1,\text{ela}}$  represent the mixing and elastic contributions, respectively.

The mixing contribution is similar to that described for systems containing a noncross-linked polymer (eq 3). In a system containing a cross-linked polymer network, the  $1/r_3$  term is negligible because the segment number of the polymer molecules is thought to be infinite ( $r_3 \rightarrow \infty$ ). For a perfect tetrafunctional network, the elastic contribution gives<sup>48</sup>

$$\Delta\mu_{1,\text{ela}} = \Delta\mu_{1,\text{ela}}^{\text{phantom}}(1 - F) + \Delta\mu_{1,\text{ela}}^{\text{affine}}F \quad (10)$$

where

$$F = K(\lambda, \kappa) / (1 - \lambda^{-2}) \quad (11)$$

and

$$K(\lambda, \kappa) = B[\dot{B}(1 + B)^{-1} + (\lambda/\kappa)^2(B + \lambda^2\dot{B}) \\ (1 + \lambda^2B/\kappa)^{-1}] \quad (12a)$$

$$\dot{B} = \frac{\partial B}{\partial \lambda^2} = B[(\lambda^2 - 1)^{-1} - 2(\lambda^2 + \kappa)^{-1}] \quad (12b)$$

$$B = (\lambda^2 - 1) / (1 + \lambda^2/\kappa)^2 \quad (12c)$$

and  $\lambda$  is the linear swelling ratio

$$\lambda = (V/V^0)^{1/3} = (\phi_g^0/\phi_g)^{1/3} \quad (13)$$

where  $V$  and  $V^0$  are the volumes of the gel network and reference state, respectively.  $\phi_g$  and  $\phi_g^0$  are the corresponding volume fractions of the gel, and the parameter  $\kappa$  is a measure of constraints on the junction fluctuations and is related to the degree of network interpenetration. The following equation can be used to determine  $\kappa$ :<sup>38</sup>

$$\kappa = (1/4)P\phi_g^0x_c^{1/2} \quad (14)$$

Here,  $x_c$  denotes the average number of segments per network chain, and the dimensionless number  $P$  is determined by the type of polymer and the molar volume of the solvent. For a specific polymer–solvent system,  $P$  remains constant, and  $\kappa$  depends only on network composition.<sup>49</sup> If fluctuations due to their embedding in the surrounding randomly configured

chains could be suppressed, then  $\kappa \rightarrow 0$ , and the real network approaches a phantom network, which is the limit of a high degree of swelling. The result from eq 12a is then  $K(\lambda, \kappa) \approx 0$  (i.e.,  $F = 0$ ), and eq 10 becomes

$$\Delta\mu_{1,\text{ela}} = \Delta\mu_{1,\text{ela}}^{\text{phantom}} = (1/2)kT(\phi_g^0/x_c)\lambda^{-1} \quad (15)$$

If fluctuations of the junctions are considered totally suppressed by the constraints,  $\kappa \rightarrow \infty$ , then the network is called an affine network, a network in which the junctions are assumed to be firmly embedded in the medium. The result from eq 12a is then  $K(\lambda, \kappa) \approx (1 - \lambda^{-2})$ , and eq 10 becomes

$$\Delta\mu_{1,\text{ela}} = \Delta\mu_{1,\text{ela}}^{\text{affine}} \\ = (1/2)kT(\phi_g^0/x_c)(2 - \lambda^{-2})\lambda^{-1} \quad (16)$$

In this work, we are concerned with networks in high dilute solutions. On the basis of the elastic contribution described above, the behavior of these networks should be close to that of the phantom network limit (i.e., we set  $P \rightarrow 0$ ).

Substituting eqs 3 and 10 into eq 9, the reduced chemical potential of a solvent in gels can be expressed by

$$\frac{\Delta\mu_1}{kT} = (1/2)(\phi_g^0/x_c)\lambda^{-1}(1 - F) \\ + (1/2)(\phi_g^0/x_c)(2 - \lambda^{-2})\lambda^{-1}F + \ln \phi_1 \\ + \left(1 - \frac{r_1}{r_2}\right)\phi_2 + \phi_g + r_1 \left[ C_\beta \left( \frac{1}{r_2} - \frac{1}{r_1} \right)^2 \right. \\ (1 - \phi_1)\phi_2 + \left( 2 + \frac{1}{r_2} \right) \tilde{\epsilon}_{12}(1 - \phi_1)\phi_2 \\ - \left( \frac{1}{r_2} - \frac{1}{r_1} + C_\gamma \tilde{\epsilon}_{12} \right) \tilde{\epsilon}_{12} \\ \times \{ (1 - \phi_1)\phi_2^2 - \phi_1\phi_2^2 \} + C_\gamma \tilde{\epsilon}_{12}^2 \\ \left. \{ (1 - \phi_1)\phi_2^3 - 2\phi_1\phi_2^3 \} \right] \\ + r_1 \left[ \frac{1}{r_1^2} C_\beta (1 - \phi_1)\phi_g + 2\tilde{\epsilon}_{13}(1 - \phi_1)\phi_g \right. \\ - \left( C_\gamma \tilde{\epsilon}_{13} - \frac{1}{r_1} \right) \tilde{\epsilon}_{13} \{ (1 - \phi_1)\phi_g^2 \\ - \phi_1\phi_g^2 \} + C_\gamma \tilde{\epsilon}_{13}^2 \times \{ (1 - \phi_1)\phi_1^3 \\ - 2\phi_1\phi_g^2 \} \left. \right] - r_1 \left[ -\frac{1}{r_1} C_\beta \phi_2\phi_g \right. \\ + 2\tilde{\epsilon}_{23}\phi_2\phi_g - 2 \left( -\frac{1}{r_2} + C_\gamma \tilde{\epsilon}_{23} \right) \tilde{\epsilon}_{23}\phi_2\phi_g^2 \\ \left. + 3\phi_2\phi_g^3 C_\gamma \tilde{\epsilon}_{23}^2 \right] \quad (17)$$

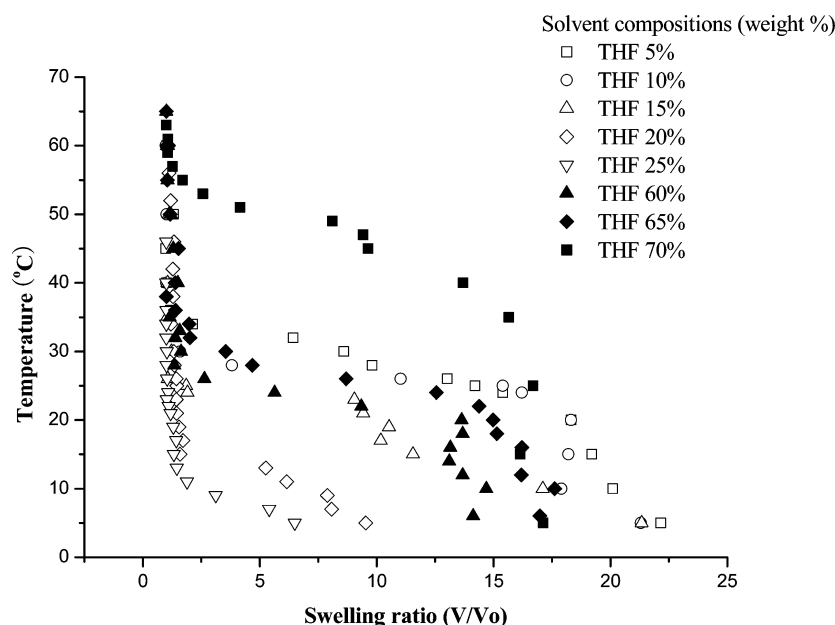


**Figure 2.** Swelling behaviors of nanometer-sized gel particles with various solvent compositions. The volume was calculated from the hydrodynamic diameter, which was measured via the PCS technique.

The equilibrium condition for a gel in a solvent system is given by

$$\frac{\Delta\mu_1}{kT} = 0 \quad (18)$$

#### 4. RESULTS AND DISCUSSION

Poly (NIPA) exhibits a well-known lower critical solution temperature (LCST) in water at about 32 °C. NIPA gel also undergoes this swelling phenomenon in water around the LCST. In mixed solvent, however, the volume transition temperature change of the NIPA gel is indicated by the ratio of solvent components. Figure 2 shows the swelling behavior of the NIPA gel particles with various water–THF compositions. To measure the swelling behaviors, the average hydrodynamic diameters,  $D_h$ , of equilibrium gels at various temperatures were measured by the PCS technique. The volume ratio of gel particles was calculated from the swelling data by the following simple relationship:

$$\frac{\phi}{\phi_g^0} = \frac{V}{V^0} = \left( \frac{D_h}{D_h^0} \right)^3 \quad (19)$$

where  $V$  is the equilibrium gel volume at the state of interest. Here, the superscript 0 in eq 19 denotes the reference state of the hydrogel, which is a synthetic condition.

The gel particles exhibited continuous volume change in the given temperature range from 0 to 65 °C. The volume transition temperature decreased with increasing THF weight fraction in the range of 5–25%, and the addition of a small amount of THF to within 60–70% increased the volume transition temperature. However, above 75%, the volume transition temperature remained constant (there was no change during the swollen state). Between a 30% and 50% weight fraction of THF, the volume transition temperature also remained constant (there was no change during the collapsed state). When the concentration of THF is low in the mixed

solvent, the hydrogen bonding that occurs between water and THF molecules disturbs the hydration between water and the NIPA gel, which promotes the hydrophobic interactions of the NIPA gel. In this region, therefore, the volume transition temperature was decreased. When the THF concentration in the mixed solvent is high, the interactions between THF and the NIPA gel are stronger than the hydrophobic interactions, causing the gel to reswell. Therefore, the volume transition temperature increases with increasing THF wt% in the THF-rich region. Mukae et al.<sup>20</sup> evaluated the swelling behavior of NIPA gel in THF (aprotic solvent)–water mixtures.

The reentrant swelling behavior was measured by computing the swelling ratio according to the weight fraction of THF within a specified temperature range. The addition of THF compounds affected the swelling of the hydrogels as well as the volume phase transition temperature.

Figure 3 is a three-dimensional representation of the swelling behaviors of NIPA gel particles in the THF–water mixture. The THF composition and swelling effects were measured, and the swelling varied with temperature as a result of different THF weight fractions. The reentrant swelling behavior of the NIPA gel particles narrowed with decreasing temperature. These behaviors indicate that the hydrogen bonding interactions between the NIPA gel and water molecules were strengthened at low THF wt %, and the THF and NIPA gel interactions became stronger at high THF wt % with decreasing temperature.

Determining the interaction energy parameters of each component may be helpful for predicting the reentrant swelling behavior of NIPA gels in mixed solvents. These parameters can be calculated from LLE data. Figure 4a shows a ternary phase diagram of water(1)–THF(2)–linear PNIPA(3) at 28 °C and the model calculation. The solid line was generated using the proposed model, and the open circles are experimental data. We set  $r_1 = 1$  for water, which is the smallest molecule in this system. The calculated model parameter values were  $r_2 = 16.02$  and  $r_3 = 159.13$ , and the interaction energy parameters were  $\tilde{\epsilon}_{12} = 23.0309$ ,  $\tilde{\epsilon}_{13} = 3.9890$ , and  $\tilde{\epsilon}_{23} = 5.8653$ .



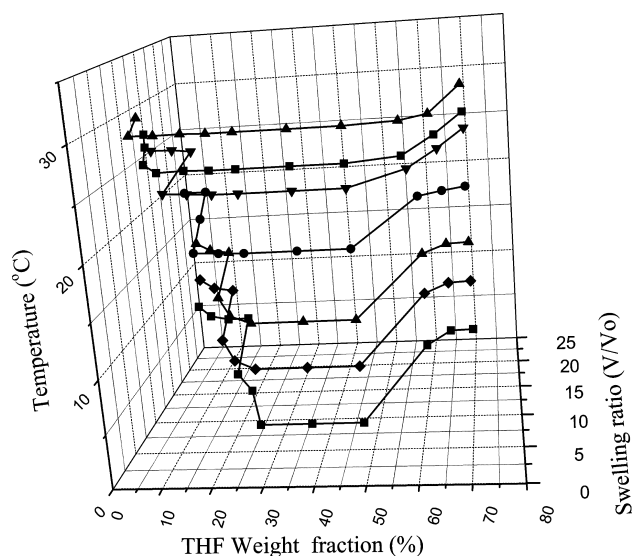


**Figure 3.** Three-dimensional representation of the swelling behaviors of NIPA gel particles in a water and THF mixture.

Figure 4b shows comparisons of the calculated swelling equilibrium with experimental data for water(1)–THF(2)–cross-linked NIPA gel(3) at  $T = 28\text{ }^{\circ}\text{C}$ . Cross-linked gels of poly NIPA that separated into two phases between 0.12 and 0.6 wt % of THF collapsed and swelled in the single-phase region as seen in Figure 3a. We applied the interaction parameters ( $\tilde{\epsilon}_{12} = 23.0309$ ,  $\tilde{\epsilon}_{13} = 3.9896$ , and  $\tilde{\epsilon}_{23} = 5.8653$ ) obtained from the proposed model to calculate swelling equilibria in the ternary system. The structural parameter,  $x_c$ , was estimated from the cross-linker density as follows:

$$x_c \approx \left( \frac{1}{2\phi_j} \right) \left( \frac{V_m}{V_s} \right) \quad (20)$$

Here  $\phi_j$  is the mole fraction of the cross-linker (or junction) unit to total monomer units in the gel network ( $\phi_j \approx$  moles of BIS in the feed solution/total moles of the monomer in the feed solution),  $V_m$  and  $V_s$  are the molar volumes of the monomer and solvent, respectively, and  $x_c$  is 256 in this system. However, the structural parameter,  $\phi_g^0$ , cannot be estimated from the experimental swelling ratio data because this system exhibits reswelling behavior. In this study, we set  $\phi_g^0$  as an adjustable model parameter for swelling data and obtained an acceptable value of 0.2. The same procedure was employed to examine the swelling behaviors at different temperatures.

Figure 5a shows a ternary phase diagram of water(1)–THF(2)–linear PNIPA(3) at  $20\text{ }^{\circ}\text{C}$ . The open circles are experimental data, and the solid line represents the calculated values of  $r_2$  and  $r_3$ , which were the same as those at  $28\text{ }^{\circ}\text{C}$ . The interaction energy parameter values were  $\tilde{\epsilon}_{12} = 20.8237$ ,  $\tilde{\epsilon}_{13} = 2.3437$ , and  $\tilde{\epsilon}_{23} = 6.8764$ . Figure 5b compares the measured and calculated swelling equilibria at  $T = 20\text{ }^{\circ}\text{C}$ . In a range of 0.17 to 0.5 wt % of THF, the system separated into two phases, and the NIPA gel collapsed. The interaction energy parameters were used directly in the calculation of the reentrant swelling equilibria. The structural parameters ( $\phi_g^0$  and  $x_c$ ) were the same as those at  $28\text{ }^{\circ}\text{C}$ .

Figure 6a shows a ternary phase diagram of water(1)–THF(2)–linear PNIPA(3) at  $32\text{ }^{\circ}\text{C}$ . The calculated interaction energy parameter values were  $\tilde{\epsilon}_{12} = 28.8237$ ,  $\tilde{\epsilon}_{13} = 5.9437$ , and

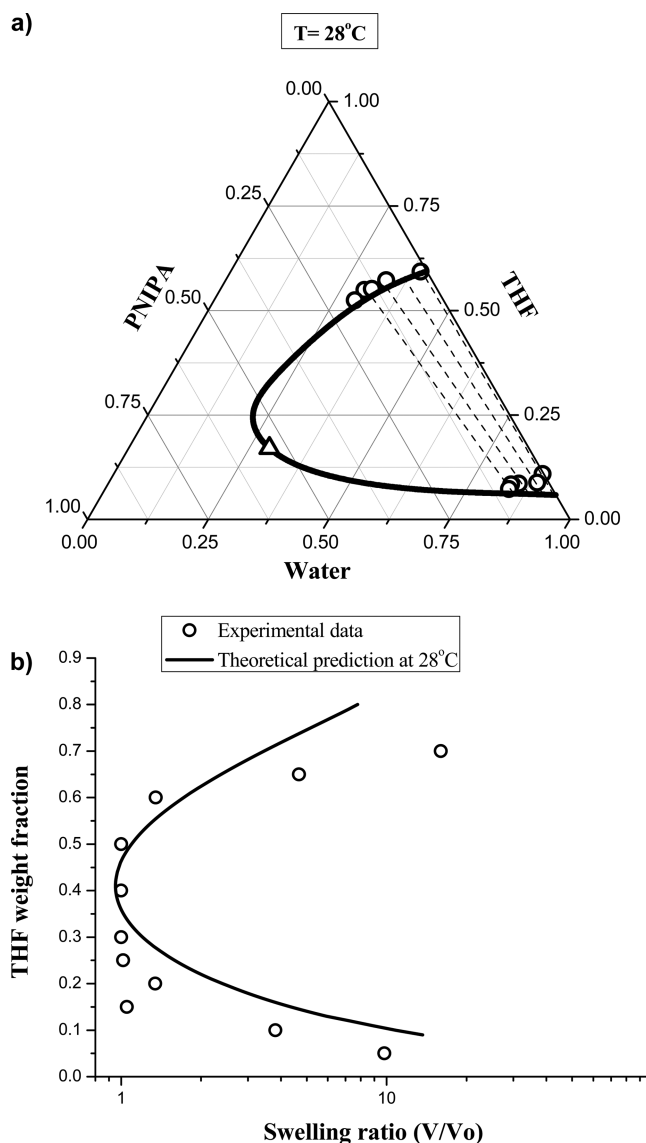


**Figure 4.** (a) Coexistence curves for the water(1)–THF(2)–PNIPA(3) ternary system showing the cloud-point as a function of the weight fraction of ternary compositions at  $T = 28\text{ }^{\circ}\text{C}$ . Solid line, calculated in this work; open circles, experimental data; open triangle, critical point. (b) Comparison between experimental swelling data of NIPA gel particles in mixtures of water and THF at  $28\text{ }^{\circ}\text{C}$  and their theoretical prediction from the proposed model. Open circles are experimental data. The solid line was generated using the proposed model.

$\tilde{\epsilon}_{23} = 7.8764$ . Figure 6b compares the measured and calculated swelling equilibria at  $T = 32\text{ }^{\circ}\text{C}$ . The NIPA gel collapsed between 0.09 and 0.65 wt % of THF, and phase separation also occurred near this region. The interaction parameters and structural parameters were the same as the above procedure.

The proposed modeling technique can help predict the gel swelling behaviors using the corresponding polymer LLE data, but limitations remained due to the inevitable fitting procedure in the calculation of ternary LLE data.<sup>50,51</sup> An improved approach is to use the molecular simulation method, which can serve as a predictive tool for solving such phase equilibrium problems. Because of the ever increasing power of computers, in recent years many scientific papers<sup>52–55</sup> have reported using combinations of the thermodynamic model and molecular

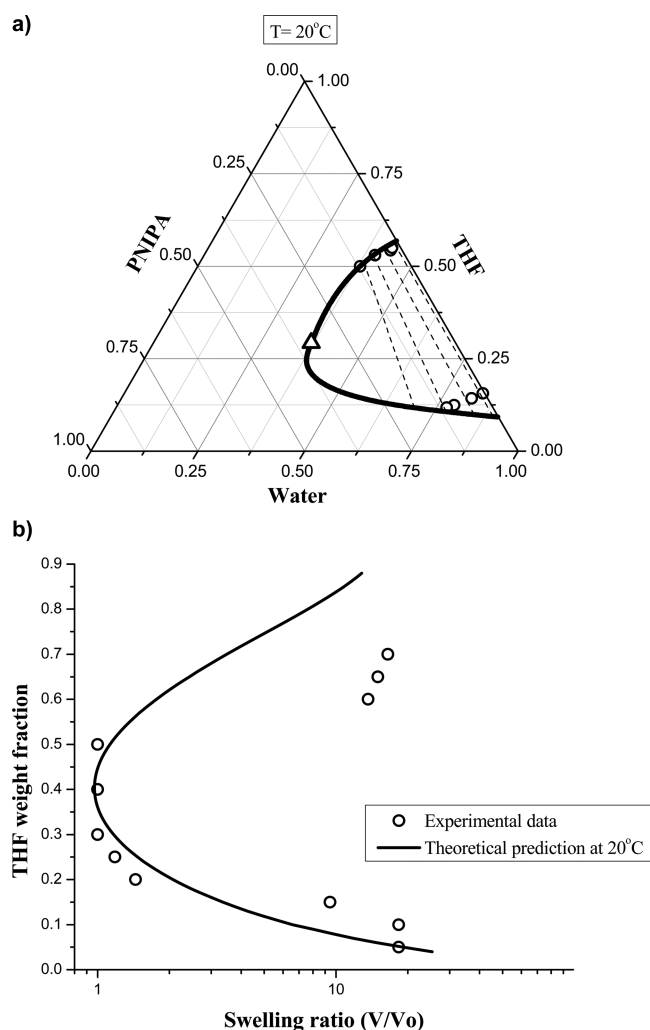


**Figure 5.** (a) Coexistence curves for the water(1)–THF(2)–PNIPA(3) ternary system showing the cloud-point as a function of weight fraction of the ternary composition at  $T = 20\text{ }^{\circ}\text{C}$ . Solid line, calculated in this work; open circles, experimental data; open triangle, critical point. (b) Comparison between experimental swelling data of the NIPA gel particles in mixtures of water and THF at  $20\text{ }^{\circ}\text{C}$  and their theoretical prediction from the proposed model. Open circles are experimental data. The solid line was generated using the proposed model.

simulations. We will apply this method to the ternary gel swelling equilibria in our future research.

## 5. CONCLUSIONS

We have shown that the thermodynamic model, through combining an MDL model for a polymer solution and the Flory–Erman elastic model, was able to describe the reentrant swelling behavior for nanometer-sized NIPA gel particles in water–THF mixed solvents. The experimentally determined cloud-point of the water–THF–linear poly NIPA systems was described using a TOA apparatus. The predetermined interaction parameters from the linear poly NIPA–water–THF ternary system were used directly to calculate reentrant swelling equilibria for the NIPA gel in mixed solvent systems. For those ternary polymer solutions, the calculation of reentrant swelling behavior is a deviation from the experimental data in the THF-rich region; however, our proposed model appears to be useful in calculating without complicated

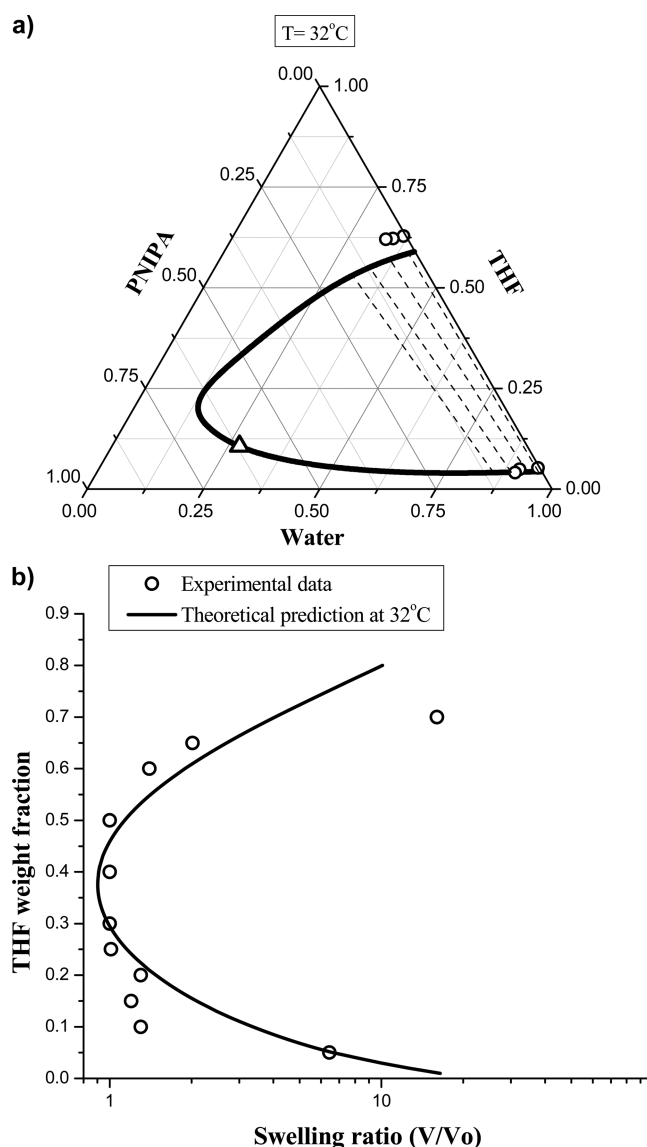


**Figure 6.** (a) Coexistence curves for the water(1)–THF(2)–PNIPA(3) ternary system showing the cloud-point as a function of the weight fraction of the ternary compositions at  $T = 32\text{ }^{\circ}\text{C}$ . Solid line, calculated in this work; open circles, experimental data; open triangle, critical point. (b) Comparison between experimental swelling data of NIPA gel particles in mixtures of water and THF at  $32\text{ }^{\circ}\text{C}$  and their theoretical prediction from the proposed model. Open circles are experimental data. The solid line was generated using the proposed model.

parameters. The advantage of this work follows from its simplicity; a simple swelling equilibria version of the MDL model appears to be suitable for predicting the reentrant swelling behavior of the given system.

## AUTHOR INFORMATION

### Corresponding Author

\*E-mail: ycbae@hanyang.ac.kr. Tel.: +82-2-2298-0529. Fax: +82-2-2296-0568.

## ACKNOWLEDGMENTS

This work was supported by the Basic Science Research Program through a grant from the National Research Foundation of Korea (NRF) funded by the Ministry of

Education, Science and Technology (MEST) of Korea for the Center for Next Generation Dye-Sensitized Solar Cells (No. 2011-0001055).

## REFERENCES

- (1) Tanaka, T. *Phys. Rev. Lett.* **1978**, *40*, 820–823.
- (2) Hirokawa, Y.; Tanaka, T. *J. Chem. Phys.* **1984**, *81*, 6379–6380.
- (3) Hirokawa, Y.; Tanaka, T.; Katayama, S. *Microbial Adhesion and Aggregation*; Springer: Berlin, 1984.
- (4) Kopecek, J.; Vacik, J.; Lim, D. *J. Polym. Sci., Polym. Chem. Ed.* **1971**, *9*, 2801–2815.
- (5) Katayama, S.; Hirokawa, Y.; Tanaka, T. *Macromolecules* **1984**, *17*, 2641–2743.
- (6) Hühner, A.; Maurer, G. *Fluid Phase Equilib.* **2004**, *226*, 321–332.
- (7) Geever, L. M.; Devine, D. M.; Nugent, M. J. D.; Kennedy, J. E.; Lyons, J. G. *Eur. Polym. J.* **2006**, *42*, 2540–2548.
- (8) Bignotti, F.; Lebon, F.; Peroni, I. *Eur. Polym. J.* **2007**, *43*, 1996–2006.
- (9) Ohmine, I.; Tanaka, T. *J. Chem. Phys.* **1982**, *77*, 5725–5729.
- (10) Irie, M.; Misumi, Y.; Tanaka, T. *Polymer* **1993**, *34*, 4531–4535.
- (11) Kokufuta, E.; Nakaizumi, S.; Ito, S.; Tanaka, T. *Macromolecules* **1995**, *28*, 1704–1708.
- (12) Hoffman, A. S. *J. Controlled Release* **1987**, *6*, 297–305.
- (13) Siegel, R. A.; Faramalzan, M.; Firestone, B. A.; Moxley, B. C. *J. Controlled Release* **1988**, *8*, 179–182.
- (14) Fornasiero, F.; Tang, D.; Boushehri, A.; Prausnitz, J. M.; Radke, C. J. *J. Membr. Sci.* **2008**, *320*, 423–430.
- (15) Amiya, T.; Hirokawa, Y.; Hirose, Y.; Li, Y.; Tanaka, T. *J. Chem. Phys.* **1987**, *86*, 2375–2379.
- (16) Hirotsu, S. *J. Phys. Soc. Jpn.* **1987**, *56*, 233–242.
- (17) Saunders, B. R.; Crowther, H. M.; Vincent, B. *Macromolecules* **1997**, *30*, 482–487.
- (18) Zhang, G.; Wu, C. *J. Am. Chem. Soc.* **2001**, *123*, 1376–1380.
- (19) Mukae, K.; Sakurai, M.; Sawamura, S.; Makino, K.; Kim, S. W.; Ueda, I.; Shirahama, K. *J. Phys. Chem.* **1993**, *97*, 737–741.
- (20) Mukae, K.; Sakurai, M.; Sawamura, S.; Makino, K.; Kim, S. W.; Ueda, I.; Shirahama, K. *Colloid Polym. Sci.* **1994**, *272*, 655–663.
- (21) Wada, N.; Yagi, Y.; Inomata, H.; Saito, S. *Macromolecules* **1992**, *25*, 7220–7222.
- (22) Liu, G. M.; Zhang, G. Z. *Langmuir* **2005**, *21*, 2086–2090.
- (23) Kumar, V.; Chaudhari, C. V.; Bhardwaj, Y. K.; Goel, N. K.; Sabharwal, S. *Eur. Polym. J.* **2006**, *42*, 2352–2354.
- (24) Gundogan, N.; Okay, O. *J. Appl. Polym. Sci.* **2002**, *85*, 801–813.
- (25) Lele, A. K.; Karode, S. K.; Badiger, M. V.; Mashelkar, R. A. *J. Chem. Phys.* **1997**, *107*, 2142–2148.
- (26) Oliveira, E. D.; Silva, A. F. S.; Freitas, R. F. S. *Polymer* **2004**, *45*, 1287–1293.
- (27) Prange, M. M.; Hooper, H. H.; Prausnitz, J. M. *AIChE J.* **1989**, *35*, 803–813.
- (28) Marchetti, M.; Prager, S.; Cussler, E. L. *Macromolecules* **1990**, *23*, 1760–1765.
- (29) Marchetti, M.; Prager, S.; Cussler, E. L. *Macromolecules* **1990**, *23*, 3445–3450.
- (30) Moerkerke, R.; Koningsveld, H.; Berghmans, K.; Dusek, K.; Solc, K. *Macromolecules* **1995**, *28*, 1103–1107.
- (31) Nandi, S.; Winter, H. *Macromolecules* **2005**, *38*, 4447–4455.
- (32) Zhi, D.; Huang, Y.; Han, X.; Liu, H.; Hu, Y. *Chem. Eng. Sci.* **2010**, *65*, 3223–3230.
- (33) Okeowo, O.; Dorgan, J. R. *Macromolecules* **2006**, *39*, 8193–8202.
- (34) Tanaka, T.; Fillore, D. J. *J. Chem. Phys.* **1979**, *70*, 1214–1218.
- (35) Oh, J. S.; Bae, Y. C. *Polymer* **1998**, *39*, 1149–1154.
- (36) Oh, K. S.; Oh, J. S.; Choi, H. S.; Bae, Y. C. *Macromolecules* **1998**, *31*, 7328–7335.
- (37) Jung, S. C.; Oh, S. Y.; Bae, Y. C. *Polymer* **2009**, *50*, 3370–3377.
- (38) Erman, B.; Flory, P. J. *Macromolecules* **1986**, *19*, 2342–2353.
- (39) Bae, Y. C.; Lambert, S. M.; Soane, D. S.; Prausnitz, J. M. *Macromolecules* **1991**, *24*, 4403–4407.
- (40) Yi, Y. D.; Oh, K. S.; Bae, Y. C. *Polymer* **1997**, *38*, 3471–3476.
- (41) Chu, B. *Laser Light Scattering*, 2nd ed.; Academic Press: New York, 1991.
- (42) Schmitz, K. S. *An Introduction to Dynamic Light Scattering by Macromolecules*; Academic Press: New York, 1990.
- (43) Tompa, H. *Polymer Solutions*; Butterworths: London, 1956.
- (44) Scott, R. L. *J. Chem. Phys.* **1949**, *17*, 268–279.
- (45) Madden, W. G.; Pesci, A. I.; Freed, K. F. *Macromolecules* **1990**, *23*, 1181–1191.
- (46) Koningsveld, R.; Staverman, A. J. *J. Polym. Sci., Part A* **1968**, *6*, 305–323.
- (47) Flory, P. J. *Principles of Polymer Chemistry*; Cornell University Press: Ithaca, NY, 1953.
- (48) Mark, J. E.; Erman, B. *Rubberlike Elasticity: A Molecular Primer*; Wiley & Sons: New York, 1988.
- (49) Hooper, H. H.; Baker, J. P.; Blanch, H. W.; Prausnitz, J. M. *Macromolecules* **1990**, *23*, 1096–1104.
- (50) Oh, S. Y.; Bae, Y. C. *Eur. Polym. J.* **2010**, *46*, 1860–1865.
- (51) Oh, S. Y.; Bae, Y. C. *Chem. Phys.* **2011**, *379*, 128–133.
- (52) Jawalkar, S. S.; Adoor, S. G.; Sairam, M.; Nadagouda, M. N.; Aminabhavi, T. M. *J. Phys. Chem. B* **2005**, *109*, 15611–15620.
- (53) Luo, Z.; Jiang, J. *Polymer* **2010**, *51*, 291–299.
- (54) Oh, S. Y.; Bae, Y. C. *J. Phys. Chem. B* **2010**, *114*, 8948–8953.
- (55) Oh, S. Y.; Bae, Y. C. *J. Phys. Chem. B* **2011**, *115*, 6051–6060.